Colloid Polym Sci (2005) 283: 783–792
DOI 10.1007/s00396-004-1226-9

Matthias Wanner
Dagmar Gerthsen
Stefan-Sven Jester
Biprajit Sarkar
Brigitte Schwederski

Treatment of citrate-capped Au colloids with NaCl, NaBr and Na_2SO_4: a TEM, EAS and EPR study of the accompanying changes

Received: 11 February 2004
Accepted: 29 September 2004
Published online: 19 January 2005

M. Wanner (✉) · D. Gerthsen
Laboratorium für Elektronenmikroskopie, Universität Karlsruhe (TH), Karlsruhe, 76128, Germany
E-mail: wanner@lem.uni-karlsruhe.de
Tel.: +49-721-6086101
Fax: +49-721-6083721

S.-S. Jester
Institut für Physikalische Chemie, Universität Karlsruhe (TH), Karlsruhe, 76128, Germany

B. Sarkar · B. Schwederski
Institut für Anorganische Chemie, Universität Stuttgart, Pfaffenwaldring 55, Stuttgart, 70569, Germany

Abstract In the present study, effects of the treatment of citrate-reduced Au sols with NaCl, NaBr and Na_2SO_4 are described. The particles are characterized by transmission electron microscopy (TEM) and spectroscopic methods, suggesting an exchange of the citrate capping by the anions of the Na salts. Under electron beam exposure the capping of the NaCl- and NaBr-treated particles disappears. The specific electronic properties of the Na salt-treated particles are studied by electron absorption spectroscopy (EAS) and electron paramagnetic resonance (EPR). A discussion of the results in comparison with the spectroscopic responses from the original particles is given. A correlation between the data of EAS and EPR is found. The respective electron-withdrawing effect of the capping anions towards the Au core seems to be of considerable significance regarding the orbital situation around the Fermi level.

Keywords Au colloids · TEM · EAS · EPR · Electronic properties

Introduction

The electronic properties of nanoscale metal particles are of interest from a fundamental and applications point of view [1–6]. Decreasing the particle diameter increases the distance between the electronic energy levels (quantum size effect) [1, 2]. Moreover, the electronic situation can also be affected by ligand molecules on the surface of the particle, which induce charge polarization of the surface atoms [7–9]. The latter is particularly found in the case of colloidal particles.

It is known that the oxyanions PO_4^{3-}, CO_3^{2-} and SO_4^{2-} have sufficiently high Lewis basicities to attack the Au core and to substitute the coating anions [9]. The colloids formed in this manner can be isolated and readily redispersed in water. Due to significant shifts of the surface plasmon resonance (SPR) bands in their electronic absorption spectrum (EAS), there is no doubt that such substitutions have an influence on the electronic situation at least concerning the atoms of the metal core surface.

No such shift of the SPR band was observed, however, when Au colloids coated with citrate and tannic acid groups were treated with NaCl [9]. In contrast to PO_4^{3-}, CO_3^{2-} and SO_4^{2-}, Cl^- does not seem to be able to attack these Au colloids to an appreciable extent at least as long as the concentration of NaCl is not increased drastically. The UV-absorption band of tannic acid also does not vanish completely in the EAS after the NaCl-treated particles were isolated from the resulting solution, leading to the conclusion that the interaction of Cl^- with Au colloids capped with citrate and tannic acid

groups has to be described as predominantly long-range electrostatic, whereas the interaction between the oxyanions and an Au surface is thought to have a significant covalent component, especially in the case of PO_4^{3-} and SO_4^{2-}, where back-donation from Au to the oxygen donor may be discussed.

In principle, a certain degree of covalency could be discussed in the interaction of Au and Cl^- as well. The phenomenon of Cl^- adsorption at Au surfaces has been well established in electrochemical studies [10] and there are several Au-Cl complexes, which are characterized by high stability constants [11]. So the main reason for the different behaviour of Cl^- anion in the experiments of Cumberland and Strouse seems to be a lack of Lewis basicity, which prevents these anions from attacking the Au core successfully shielded by citrate **and** tannic acid groups. Since tannic acid is to be regarded as a relatively bulky, high-molecular weight compound, a different behaviour could be expected from the treatment of exclusively citrate-capped Au colloids with NaCl.

Here, we present some characteristic properties of particles, which were prepared by treatment of the well-known citrate-capped Au colloids with NaCl as well as with NaBr and Na_2SO_4. Some striking effects become obvious when using TEM, EAS and low temperature EPR spectroscopy as methods to characterize these particles. Comparing these results with those obtained from the original Au sol, the different behaviour can be explained by means of specific variations in the electronic structure of these particles.

The characterisation of salt-treated colloidal systems, as presented in this work, may therefore contribute to manage the tuning of the electronic properties of colloidal nanoparticles by purposeful selection of the capping anions in the same way as by variation of their size or the core's chemical composition. This widens the field of parameters and may be applied, e.g. in order to synthesize particles with desired optical or magnetic properties.

Experimental

Colloid formation

The aqueous Au sol consisting of app. 15 nm-diameter Au particles was prepared similar to the method of Turkevich et al. [12] 5 mg (2.3×10^{-5} mol) chloroauric acid (Alfa Aesar, 99.99%) was solved in 95 ml of distilled water and heated. Stirring vigorously, 5 ml (2.3×10^{-4} mol) of an aqueous 0.9%-solution of citric acid (Merck) was added rapidly to the boiling solution. After about 15 s the liquor turned from colourless to purple. Addition of 35 mg (6.0×10^{-4} mol) of NaCl to 10 ml of the prepared Au sol at room temperature caused a change in colour to lavender (5 min) and finally to greyish-blue (20 min). The treatment of the Au sol with anhydrous Na_2SO_4 and NaBr was carried out similarly.

Transmission electron microscopy (TEM)

The TEM was performed with a Philips CM200 FEG/ST electron microscope at an electron energy of 200 keV equipped with a Noran Ge detector system for energy-dispersive X-ray analysis (EDX).

Electron absorption spectroscopy (EAS)

Electron absorption spectroscopy was carried out using a Varian CARY 5E UV-Vis-NIR spectrophotometer (intrinsic resolution 1 nm) and 1 ml quartz cuvettes ($d = 2$ mm).

Electron paramagnetic resonance (EPR) spectroscopy

Electron paramagnetic resonance spectra of frozen Au sols as well as of solids in SUPRASIL quartz tubes were recorded in the X band on a Bruker System ESP 300e equipped with a Bruker ER035 M gaussmeter and a HP 5350B microwave counter. An Oxford Instruments cryostat ESR 900 was used for measurements at liquid He temperatures.

Sample preparation

The samples for TEM investigations were prepared by dropping the Au sols through holey carbon films (thickness about 10 nm) mounted on copper grids, which were placed on absorbent material. The solid-state samples for EPR spectroscopy were prepared as follows: slow evaporation of about 5 ml of the Au sol in an inclined beaker containing the substrate resulted finally in high particle densities on the humid material. Cotton threads and cellulose stripes were used as substrate. The substrate material itself as well as that impregnated with the salts was found to be EPR-silent at liquid He temperatures.

Results and discussion

TEM

A TEM micrograph of a sample prepared from the original sol of the citrate-capped Au colloids is shown in Fig. 1a. The sample contains predominantly multiply twinned particles (MTPs), but also some ''triangular''

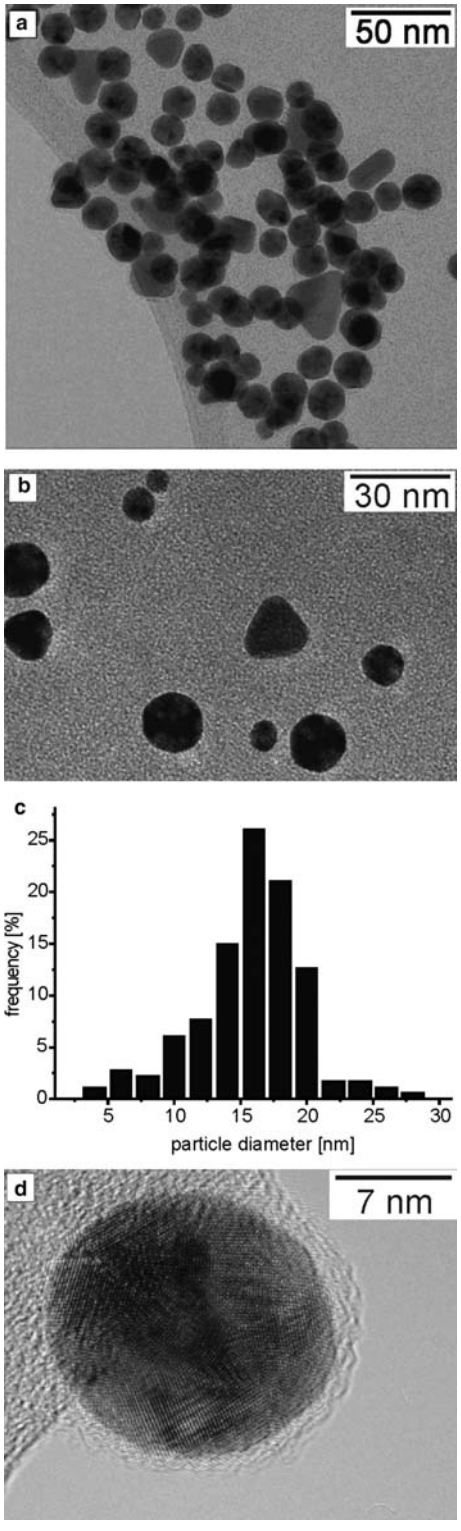

Fig. 1 TEM micrograph of the citrate-capped Au colloids after **a** five-times **b** one-time "filtration" of the Au sol through the holey carbon film. **c** Histographic size distribution. **d** Icosahedral particle with capping

(7%) and some rodlike (2%) particles. To achieve the density of particles shown, it was necessary to use the carbon support film five times as a "filter" for the Au sol (cf. preparation). Due to the flow direction of the effluent sol, the particles are concentrated around the holes of the carbon film. If the carbon film is treated with the Au sol only once, the particle density is observed to be significantly lower and it becomes apparent that there is no significant particle aggregation (Fig. 1b). As a rule, the particles do not overlap each other in this case. The columns in Fig. 1c show the histographic size distribution. Triangular and rodlike particles were not taken into account in this statistical analysis.

Observing particles, which extend over the edge of the carbon support into the vacuum, it is possible to distinguish between core and coating (Fig. 1d). Such a coating was found around each particle without exception and its thickness never deviated from the range of 1–3 nm. We attribute the coating to layers of at least partly deprotonated citric acid molecules or their oxidized products (e.g. acetone dicarboxylic acid) [12].

Particles from the NaCl-treated Au sol (cf. synthesis) show different features. As is obvious from Fig. 2a, a generally much larger degree of particle aggregation seems to be present. Although only one drop of this Au sol was used for preparation of this sample, the particles tend to be overlaid even more strongly than shown in Fig. 1a. Moreover, it can be observed that the coating of the particles is not persistent in the electron beam. Figure 2b shows the typical stepwise disappearance of the coating under continuous influence of the electron beam. These images were taken after delays of about 2 min each. In contrast, the coatings of the original particles seem to be completely resistant towards the influence of the electron beam under comparable conditions. These findings may be explained by the specific properties of these two anions concerning their function as capping agents towards metal particles.

Cl^- is a monodentate ligand, whereas citrate [13] as well as various other anions like SO_4^{2-}, CO_3^{2-} and PO_4^{3-} [9] act as bidentate or polydentate ligands towards the Au surface. So, the lack of a stabilizing chelate-effect may be one initializing reason for the observation shown in Fig. 2b. Mechanistically, one can assume that in the first step the electron beam causes the formation of chlorine radicals. In the second step, two of those radicals combine to a Cl_2 molecule, which desorbs from the Au surface into the vacuum. As one would expect, a similar phenomenon is observed in the case of NaBr-treated and (as previously described [14]) in the case of NaI-treated particles.

The gradual loss of the capping facilitates high resolution (HR) TEM observations, since the signal to noise ratio becomes larger if the amount of amorphous material around the observed particle is reduced.

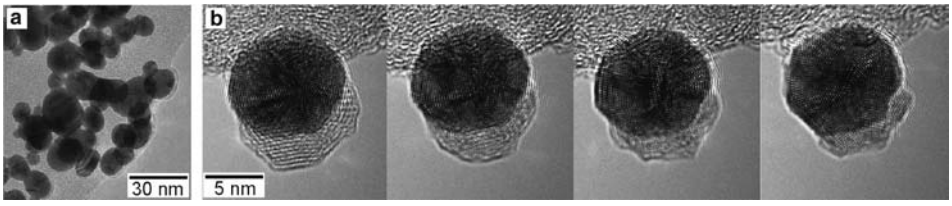

Fig. 2 TEM micrograph of NaCl-treated Au colloids **a** after one-time "filtration" of the Au sol through the holey carbon film. **b** Disappearance of the capping under electron beam exposure ($\Delta t = 2$ min each)

Figure 3a shows an HRTEM image of a particle from the NaCl-treated Au sol, whose capping has already started to disappear. As in all cases observed, here the power spectrum suggests the presence of a multiply twinned particle (MTP) structure. In more detail, it fits well with an MTP with more than one centre. A larger distance from the centre in the power spectrum is observed for some reflections (see arrows), which is typical for the case of a decahedral MTP. In such a species, the average lattice spacings are modified due to the larger gap in the incoherent twin boundaries [15]. The described reflections at larger reciprocal spacing were observed at least for all cases, in which such a small particle was oriented close to the fivefold axis.

After the complete loss of the capping, the particles show a various dynamic behaviour. Under exposure of the electron beam, the structure may change from the originally observed MTP- to the single crystal fcc-type. The images shown in Fig. 3b–e were taken after delays of 1 min each and display such a "naked" fcc-type cuboctahedral particle oriented along close to [110] (Fig. 3b, c, e) and close to [001] (Fig. 3d). Structural rearrangements occur (Fig. 3b, c) [16] and the particle rotates and moves under electron beam exposure (Fig. 3d, e).

EAS

Electron absorption spectra were taken from the Au sols of the original and the NaCl-treated particles (Fig. 4a). The original sol is characterized by an SPR absorption maximum at $\lambda = 524 \pm 1$ nm. This is in the typical range for Au particles coated under the participation of citrate. The literature data are, e.g. $\lambda = 521$ nm [17] and $\lambda = 525$ nm [9]. Quantum size effects may have a certain influence on λ although they are calculated to be rather small. Following the classical optical theory, the absorption maxima for uncoated Au clusters were calculated to be 522.5 ± 1 nm [18] for particle sizes ranging between 16 and 3 nm. Note, however, that in several cases a significantly stronger particle-size dependence of the SPR-absorption maximum has been observed in experiment, especially in the lower size range [19–22]. For instance, Kaifer et al. [20] report λ-values from 507 to 520 nm for cyclodextrin-coated Au particles in the size range of 2.7–6.4 nm, respectively.

After curve analysis including background correction, the SPR absorption maxima of the spectra of our Au sols, which were treated with increasingly larger amounts of NaCl (see Fig. 4a, broken lines), were measured to 525 ± 1, 531 ± 1 and 538 ± 1 nm for NaCl concentrations of 3×10^{-2}, 5×10^{-2}, 7×10^{-2} M, respectively.

Due to the fact that the spectra of the Au sols exhibit an increasing red-shift of the SPR band if NaCl is added gradually, this shift cannot be attributed to size effects.

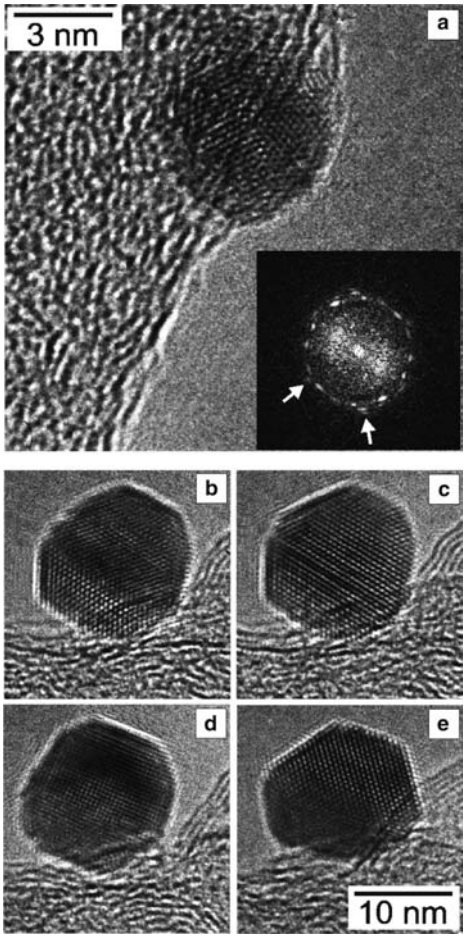

Fig. 3 **a** TEM micrograph of one small particle, whose capping has not already disappeared. Its power spectrum (see text) is shown in the *bottom*. **b–e** A series recorded from one particle after complete disappearance of the capping ($\Delta t = 1$ min each)

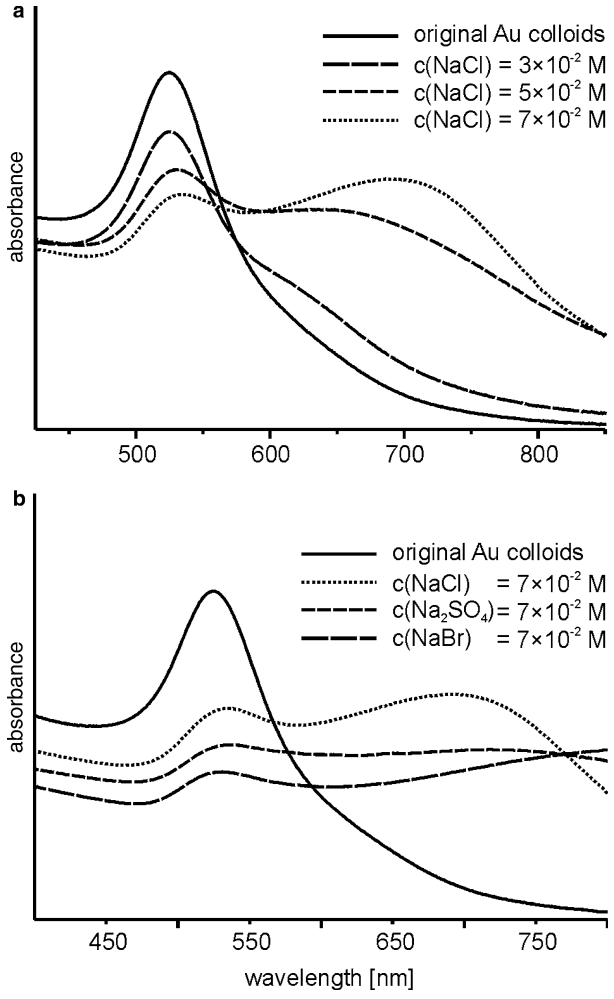

Fig. 4 EAS spectra of the treatment of the Au sol with **a** different concentrations of NaCl **b** different Na salts ($c = 7\times10^{-2}$ M)

The size distribution of the Au particles in the samples was found to be unchanged. Thus, the shift of the plasmon resonance band from 524 up to 538 nm results from a variation of the stabilizing ligand shell or from modification of the core charge state.

Mulvaney et al. [18] performed spectroelectrochemical investigations from which they deduced a direct correlation between the electrochemical potential and the λ-shift of the plasmon band. They used thiolate-protected Au particles with a mean diameter of 5.2 ± 0.2 nm from which they observed absorption maxima at 516, 520 and 525 nm at potentials of -0.16, $+0.60$, $+0.82$ V versus a Ag quasi-reference electrode, respectively. With reference to Mie theory [23, 24], the authors concluded that a decrease of the free electron concentration in the metal core results in a red-shift of the surface plasmon band.

The free electron concentration in the metal core can also be influenced by the exchange of the ligand shell, which was clearly demonstrated by Cumberland and Strouse [9]. Substitution of the citrate/tannic acid ligand shell by SO_4^{2-}, CO_3^{2-} and PO_4^{3-} resulted in a shift of the surface plasmon band from 525 to 534, 536 and 544 nm, respectively. In our experiment, we observed a comparable red-shift of finally 14 nm (c(NaCl) = 7×10^{-2} M).

All these red-shifts may be explained by stronger positively charged Au centres at the surface of the particles caused by the more pronounced electron-withdrawing influences of these "inorganic" anions [9, 18] and by gradually smaller covalent contributions to the metal-to-ligand bond.

In the experiments of Cumberland and Strouse, EAS spectra were recorded for particles, which were isolated and redispersed after treatment with the Na salts [9]. In contrast, all the spectra shown in this study were recorded directly from the salt-treated Au sols. In order to compare our EAS data with the referenced results, we also performed an EAS investigation with a Na_2SO_4-treated Au sol (Fig. 4b). After curve analysis including background correction, the resulting SPR absorption maximum is located at 534 ± 1 nm, which is in good agreement with the data from the isolated and redispersed particles (534 nm) [9]. In addition, the EAS spectrum of a NaBr-treated Au sol was recorded, from which we obtained an SPR absorption maximum of 530 ± 1 nm. The EAS data are summarized in Table 1. Trends in SPR maximum may be explained by the specific nature of the metal-to-ligand bond. Br is characterized by a moderate electronegativity and Br^- is comparatively large; a significant extent of back-donation can be discussed. So, this "soft" anion should exhibit a rather covalent interaction towards the Au centre. In the case of Cl^- and SO_4^{2-}, the electronegativity of the coordinating atoms is very high, but due to the charge SO_4^{2-} can be expected to be less electron-withdrawing than Cl^- . Thus, the NaCl-treated particles show the strongest red-shift.

Moreover, the data show a correlation between the values of the SPR absorption maxima and the observed agglomeration bands (λ(aggl.) > 600 nm) [27]. The broadening of the agglomeration band indicates a broader distribution concerning the dimensions of the

Table 1 Experimental EAS and EPR data of L-treated colloidal particles. $\zeta(L)$ is the spin-orbit coupling parameter of the respective atom. The EAS data refer to $c(L) = 7\times10^{-2}$ M

L	λ(SPR)/nm	λ(aggl.)/nm	Δg, $< g >$ [a]	ζ (L)/cm^{-1} [25, 26]
Cl^-	538	~690	< 0.001, 2.0029	587
SO_4^{2-}	534	~720	0.265, 2.161	S: 382, O: 151
Br^-	530	> 800	–[b]	2460

[a] Calculated from $\Delta g = g_1 - g_3$ and $< g > = [1/3(g_1^2 + g_2^2 + g_3^2)]^{1/2}$
[b] Not observed

particle aggregates, whereas a lower-energy absorption maximum points to increasingly denser aggregates [21, 27]. Thus, the observed increasing red-shift of the agglomeration band of the Cl^- -, SO_4^{2-} - and Br^--treated particles, respectively (Fig. 4b, Table 1), may reflect the decrease of the particle charge state, since the phenomenon of particle aggregation is ascribed to greater van-der-Waals-attraction in comparison to Coulomb-repelling forces [21]. A further example of the contest between repelling and attractive forces is the observation of Henglein and coworkers [28], that Au particle condensation is enhanced if the concentration of citrate is reduced. Moreover, the extent of aggregation of citrate-reduced particles can be enhanced if pH is lowered [27].

Recently, Jullien and coworkers [29] used NaCl-induced aggregation as a method to obtain insight into the steric protection of different capping agents on Au particles. In the case of poly-*N*-[tris-(hydroxymethyl)methyl]acrylamide as capping agent, they observed a decrease in the intensity of the plasmon resonance band and its shift from 523 to 536 nm as well as a pronounced shoulder at the lower wavelength side after addition of 5 M aqueous NaCl. Although these results seem to agree well with our data, it has to be pointed out that in our experiment with citrate as capping agent a concentration of just 6×10^{-2} M was found to be sufficient to induce coagulation (cf. Colloid formation), whereas a concentration of 3×10^{-2} M aqueous NaCl resulted in no significant change of colour even after a delay of 30 min. In this context, it seems to be remarkable that NaCl concentrations of at least 5×10^{-2} M were found to be necessary to induce coagulation even in the case of Au particles prepared by vacuum evaporation (i.e. particles without any steric protection) [30]. Thus, one may conclude that the citrate coating is not an effective shield against Cl^--attack. In contrast, if a mixture of citrate and the more bulky tannic acid is used as reducing agents, as described previously, Cl^- seems unable to attack the Au core sucessfully, since no SPR band shift can be observed [9]. Thus, merely electrostatic interaction is discussed in this case; the original coating is found to remain on the Au surface according to spectroscopic results.

EPR

In EPR spectra taken at 3.6 K, no detectable EPR response was gained from the frozen Au sols. This was observed for the original citrate-capped particles and for the particles treated with Na salts. Moreover, the substrate-deposited samples, characterized by an increased particle density (cf. preparation), prepared from the original and the NaBr-treated particles were found to be EPR silent at 3.6 K. In contrast, the substrate-deposited samples of the Au sols treated with NaCl and Na_2SO_4 induced sufficiently intensive EPR signals. Both spectra are shown in Fig. 5. The NaCl-treated sample caused an isotropic EPR signal ($g = 2.0029$), which could be simulated by gaussian lineshape and a linewidth of 0.61 mT. An EPR signal characterized by such a linewidth and *g*-value could be due to an organic radical, but at room temperature no signal was obtained from this sample. Thus, an organic impurity cannot be the source of the spectrum. In the same way, the Na_2SO_4-treated sample was found to be EPR silent at room temperature. Simulation of its spectrum taken at 3.6 K resulted in a rhombic signal ($g_1 = 2.327$, $g_2 = 2.087$, $g_3 = 2.062$) of lorentzian lineshape and significantly larger linewidths ($LW_1 = 33.0$ mT, $LW_2 = 6.5$ mT, $LW_3 = 3.9$ mT).

Several EPR experiments with heavy-metal particles are described in the literature, which gave low-width EPR signals located at *g*-values close to g_e[31–34]. Other

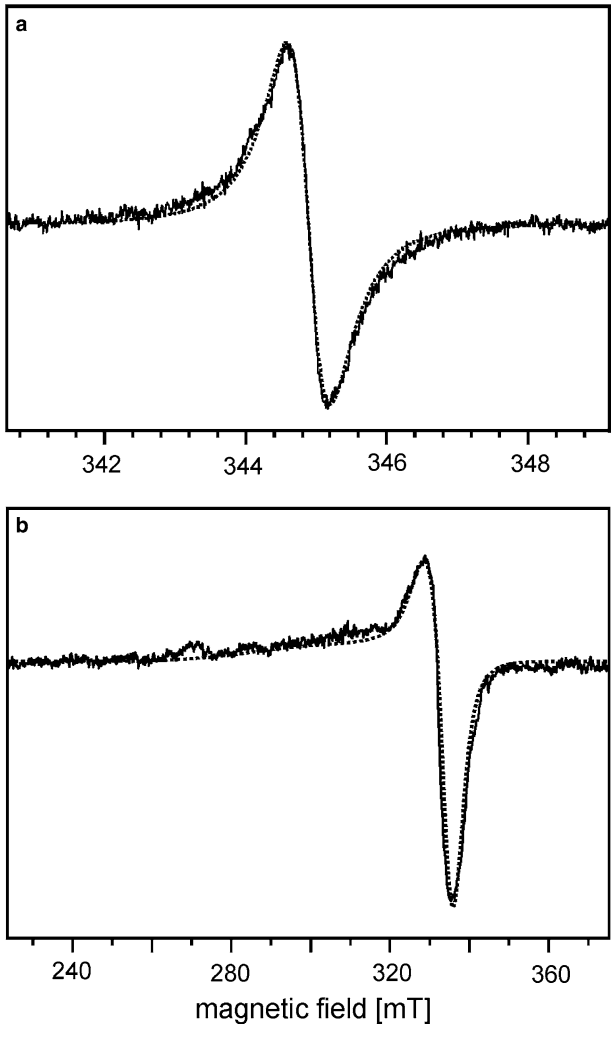

Fig. 5 X band EPR spectrum ($T = 3.6$ K) of the substrate-deposited Au particles treated with **a** NaCl, **b** Na_2SO_4. The *dotted lines* represent the computer simulation

experiments did not show any EPR response from heavy-metal particles even at low temperature [35], and a third fraction showed signals characterized by certain degrees of line broadening as well as noticeable g-shifts [36, 37]. Thus, different aspects have to be taken into account to explain the specific EPR results.

The spin-orbit coupling parameter of gold is quite large. Therefore, a significant extent of line broadening, due to high spin relaxation rates, has to be expected even at low temperature [35]. Quantum size effects can inhibit relaxation phenomena in small particles and some theoretical studies have been carried out in the last decades [2, 38–42]. According to these models, the following parameters may affect the relaxation behaviour in metal particles:

Particle size

According to Kubo [41], the level spacing of quantized electronic states becomes larger with decreasing particle size in small particles. Due to the loss of the "continuous" energy band with a high density of states, which is characteristic of bulk material, relaxation processes are inhibited in small particles. In general, such effects are discussed if $\delta >> k_B T$, where δ is defined as the average difference of the energy levels around the Fermi energy [2, 41, 42]. Halperin [2] introduced some "straight lines" (logarithmic scaling), for which the condition $\delta = k_B T$ is fulfilled, calculated for different metals (Fig. 6). For Au particles at 3.6 K, the temperature of our EPR experiment, $\delta = k_B T$, is fulfilled for particles of a size of about 17 nm. So, at least our smallest particles could fulfil the condition $k_B T << \delta$ at 3.6 K.

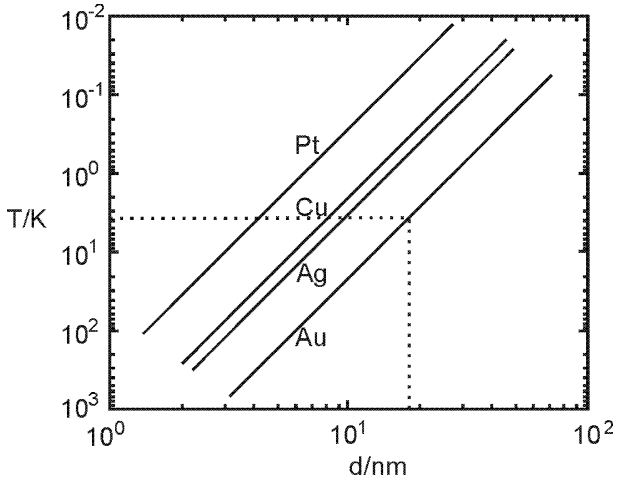

Fig. 6 Average electron-level spacing as a function of the particle diameter for a selection of metallic elements following Halperin [2]. The *straight lines* fulfil the condition $\delta = k_B T$. The *dotted line* gives the information that at 3.6 K, $\delta = k_B T$ is fulfilled for 17 nm Au particles

Particle shape

Not only the particle size, but also its shape should have a significant effect on the energy-level situation [43]. Kubo's as well as Kawabata's theories are based on the model of a spherical particle, although small irregularities are necessary to remove degeneracy [41]. Icosahedral and cuboctahedral particles may fulfil this condition formally, especially after energy minimization by surface-relaxation processes [44, 45]. Note that decahedral particles, at least if they are not truncated [46, 47] substantially, should not be regarded as spherical particles in the same manner. Moreover, it is well known that the multiply twinned particles consist of fcc-tetrahedra, which cannot fill the shape ideally. This results either in the distortion of the fcc-tetrahedra or in the toleration of a gap of about 7° in the particle [48–50]. In both cases, the energy-level situation clearly should be affected by such defects and would therefore deviate from the situation in comparable spherically shaped single crystals.

Particle environment

First, there may be an interaction between the particles and the substrate. This kind of interaction is able not only to affect the electronic but even the atomic structure at least of small particles [51, 52]. In some cases, it was observed that such influences become strong enough to make the particles become flat [53]. We suppose such effects to be rather small in our case, since the capping of our particles should prevent them from interacting with the substrate to a considerable extent. Moreover, we found by TEM investigation that the average thickness of the capping did not deviate significantly between the original sample and the particles treated with the Na salts (cf. Fig. 1d, 2b). So, significantly different extents of interaction between the substrate and the diversely capped particles are considered to be unlikely and should therefore not be regarded as the reason for the specific EPR results.

Secondly, the degree of interaction of the particles among each other affects the energy level situation, as can be seen from EAS. For instance, Quinten and Kreibig [21] describe specific variations concerning the agglomeration bands ($\lambda > 600$ nm) due to the extent and to the aggregate type of agglomeration. Although in our case the density of particles on the substrates, investigated by EPR spectroscopy, is to be considered much higher than that observed on the carbon film in TEM, differences regarding the particle aggregation in the substrate samples of the salt-treated particles and the original citrate-capped particles may pertain. So, indeed the differences concerning the particle aggregation behaviour in these Au sols could contribute to the specific EPR result to a certain extent. Note that no direct correlation can be determined between EAS data

regarding particle aggregation and specific EPR results (cf. Table 1). The original particles are characterized by a completely missing agglomeration band, whereas the EAS data of the NaBr-treated samples indicate dense aggregates. However, the EPR investigation of samples from these two Au sols resulted in no signal. Thus, we conclude that the phenomenon of particle aggregation, at least in itself, is not crucial regarding its impact on EPR signals or relaxation rates.

Particle charge

Kubo's theory is valid exclusively in the case of neutral particles. Even the charge of only one electron in particles of 10^4 atoms results in an energy difference, that is by far larger than k_BT at low temperatures [42, 54, 55]. However, charged particles can be discussed even at low temperature, if they are stabilized by chemisorption of counterionic species, since typical chemisorption bond energies are calculated to overwhelm the amount of energy necessary for ionisation [7, 8, 56]. In these cases, the energy level distances will be strongly affected [7, 8]. Thus, a significant diminution of electron density regarding the surface atoms of the Au cores, which for the NaCl-treated particles and Na_2SO_4-treated particles can be deduced from our EAS data (cf. Table 1), may be one important reason for the result that the original citrate-capped and the NaBr-treated particles were found to be EPR-silent, whereas samples from the two other fractions were EPR-active.

Spin-orbit coupling

It is well known that the spin-orbit coupling constant of the core atoms has considerable effect on the relaxation behaviour of small particles [40]. Moreover, one could assume that also the spin-orbit coupling parameters of the ligand atoms could have some influence at least in these cases in which the ligand atoms interact with the relevant orbitals of the cluster to some extent. Such interactions are known, e.g. for borate cluster radical anions. As obvious from Table 2, there is a definite correlation between the spin-orbit coupling of the coordinating halogens and the g-shift as well as the anisotropy of the signal. In these systems, increasing g-shifts and anisotropies are intimately connected with line broadening [57], which aggravates the detection of the signal of species with heavy ligand atoms even at low temperatures. Thus, a further reason for the finding of "EPR-silent" NaBr-treated particles may be line broadening due to the larger spin-orbit coupling constant of bromine.

The value of δ also affects the susceptibilty of the sample. Sone [61] found that the susceptibilty at low temperatures should decrease in the case of particles with an even number of electrons ("even particles"), whereas it should increase in the case of odd particles. These deviations from Pauli-paramagnetic behaviour are limited to the condition $k_BT < \delta$, which is fulfilled at 3.6 K as previously described for Au particles, which are smaller than 17 nm in diameter. The extent to which such deviations from Pauli-paramagnetic behaviour can be expected depends strongly on the value of ρ (see Fig. 7). According to Halperin [2] ρ can be approximately calculated as $\rho \approx h v_F (\Delta g_\infty)^2/(6\delta d)$, where $v_F$is the Fermi velocity, Δg_∞ is the g-shift of the bulk compound, δ is the average difference of the energy levels around the Fermi energy and d is the particle diameter. The Fermi velocity in gold is around 1.4×10^6 ms^{-1} [62] and Δg_∞ was determined experimentally to be about 0.1 [63]. Following Michalik et al. [32], δ can be calculated as $\delta = 2\, m_e {v_F}^2/(3n(\pi/6)d^3)$, where m_e is the mass of the electron, d is the particle diameter and n is the density over atomic mass times Avogadro's number. So, for gold at 3.6 K n, is about 5.95×10^{28} m^{-3} . Inserting Michalik's equation in Halperin's, one gets ρ as a function of d. Since Halperin points out that his equation is valid exclusively in the case of small particles, the calculation is done for particle diameters from 1 to 4 nm. This results in ρ-values of about 0.04, 0.16, 0.36 and 0.65, respectively, which means that a certain amount of increase in susceptibilty has to be expected in those cases where an odd number of electrons is present in the particles and for which $k_BT < \delta$ is fulfilled. This Curie-like behaviour at low temperatures may explain the finding, that it was possible to gain a sufficiently intensive EPR response from our NaCl- and Na_2SO_4-treated particles at 3.6 K, whereas at room temperature no detectable intensity was received from these samples.

Table 2 Spin-orbit coupling parameters ζ (L) in comparison to g factor data experimentally obtained from perhalogenated boron cluster anions

L	Δg, $< g >$[a] in $B_6L_6^{\cdot-}$ [58]	Δg, $< g >$[a] in $B_9L_9^{\cdot-}$ [59]	Δg, $< g >$[a] in $B_{12}L_{11}^{\cdot-}$ [60]	ζ (L)/cm^{-1} [25]
Cl	< 0.01, 2.027	< 0.01, 2.019	–[b]	587
Br	0.27, 2.043	0.05, 2.080	0.015, 2.004	2460
I	0.89, 1.657	0.32, 2.191	0.019, 2.008	5060

[a]Calculated from $\Delta g = g_1 - g_3$ and $< g > = [1/3({g_1}^2 + {g_2}^2 + {g_3}^2)]^{1/2}$
[b]Not determined

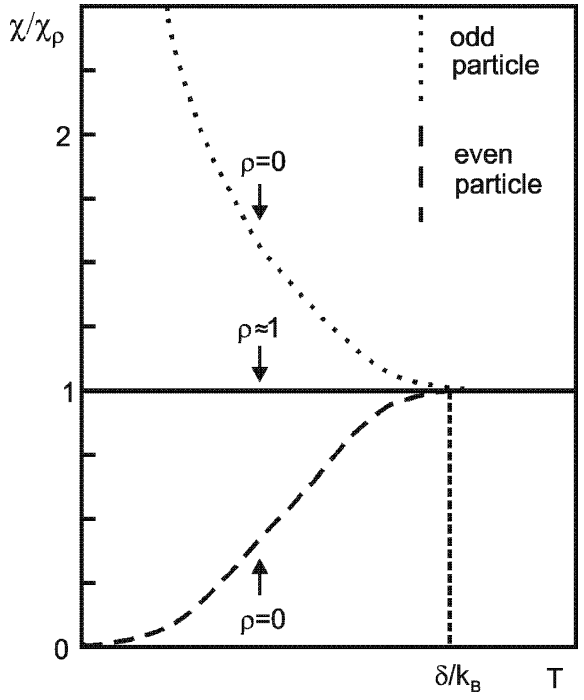

Fig. 7 Susceptibilty as a function of the temperature as calculated by Sone [61] in an equal level spacing approximation. ρ is a material-dependent constant (see text)

Conclusion

The coating of citrate-reduced Au colloids can be substituted by treatment of the sol with NaCl, NaBr and Na_2SO_4. Since the halogenides are monodentate ligands and Hal_2 is volatile, the coating of these particles can be removed under the influence of the electron beam.

The gradual substitution of the capping leads to progressive red-shifts of the SPR band, indicating the stronger electron-withdrawing effect of the Cl^--ligand. Among the anions Cl^-, SO_4^{2-} and Br^-, Cl^- seems to be the strongest and Br^- the weakest electron-withdrawing ligand towards the Au core. This ranking may play a certain role regarding the finding that the original citrate-capped particles and the NaBr-treated particles are found to be EPR-silent, whereas an EPR signal at liquid He temperatures is obtained from the SO_4^{2-}- and the Cl^--treated particles. This is the first time that EPR spectra from Au colloids are observed. The EPR results suggest larger distances of the energy levels around the Fermi level in the case of the SO_4^{2-}- and Cl^--treated particles, since due to theory an increase in susceptibility as well as a decrease in relaxation rates have to be expected in those cases in which $\delta >> k_B T$ is valid.

In this paper, we have shown that it is possible to significantly "tune" the properties of given colloidal particles by exchange of their capping. The consequences usually caused by size effects can in principle be reproduced by such substitutions at least in cases in which a situation $\delta \approx k_B T$ is given. Therefore, further experimental investigations are required for particles that fulfil this condition according to Halperin's straight lines, in order to confirm the information gained in this work.

Acknowledgements MW thanks M.M. Kappes for instructive discussions. This work has been funded by the Center for Functional Nanostructures (CFN), which is a research centre of the Deutsche Forschungsgemeinschaft (DFG).

References

1. Perenboom JAAJ, Wyder P, Meier F (1981) Phys Rep 78:173
2. Halperin WP (1986) Rev Mod Phys 58:533
3. Lue J-T (2001) J Phys Chem Sol 62:1599
4. Shipway AN (2000) ChemPhysChem 1:18
5. Henglein A (1997) Ber Bunsenges Phys Chem 101:1562
6. Kamat PVJ (2002) Phys Chem B 106:7729
7. Harris JG, Painter GS (1976) Phys Rev Lett 36:151
8. Messmer RP, Salahub DR (1977) Phys Rev B 16:3415
9. Cumberland SL, Strouse GF (2002) Langmuir 18:269
10. Lingane JJ (1962) J Electroanal Chem 4:332
11. Finkelstein NP, Hancock RD (1974) Gold Bull 7:72
12. Turkevich J, Stevenson PC, Hillier J (1951) Discuss Faraday Soc 11:55
13. Sandroff CJ, Herschbach DR (1985) Langmuir 1:131
14. Wanner M, Gerthsen D (2004) Colloid Polym Sci 282:1126
15. Urban J, Sack-Konghel H, Weiss K (1993) Z Phys D 28:247
16. Smith DJ, Petford-Long AK, Wallenberg LR, Bovin J-O (1986) Science 233:872
17. Biggs S, Chow MK, Zukoski CF, Grieser F (1993) J Coll Interf Sci 160:511
18. Templeton AC, Pietron JJ, Murray RW, Mulvaney PJ (2000) Phys Chem B 104:564
19. Pileni MP (1993) J Phys Chem 97:6961
20. Liu J, Ong W, Roman W, Lynn MJ, Kaifer AE (2000) Langmuir 16:3000
21. Quinten M, Kreibig U (1986) Surf Sci 172:557
22. Doremus RH (1964) J Chem Phys 40:2389
23. Ung T, Giersig M, Dunstan D, Mulvaney P (1997) Langmuir 13:1773
24. Mie G (1908) Ann Phys 25:377
25. McClure DS (1949) J Chem Phys 17:905
26. Morton JR, Rowlands JR, Whiffen DH (1962) National Physical Laboratory (UK) Circular No. BPR 1.3
27. Shipway AN, Lahav M, Gabai R, Willner I (2000) Langmuir 16:8789
28. Henglein A, Giersig M (1999) J Phys Chem B 103:9533

29. Mangeney C, Ferrage F, Aujard I, Marchi-Artzner V, Jullien L, Ouari O, Rekai ED, Laschewsky A, Vikholm I, Sadowski JW (2002) J Am Chem Soc 124:5811
30. Thompson DW, Collins IR (1994) J Coll Interf Sci 163:347
31. Monot R, Châtelain A, Borel J-P (1971) Phys Lett 34A:57
32. Michalik J, Brown D, Yu J-S, Danilczuk M, Kim JY, Kevan L (2001) Phys Chem Chem Phys 3:1705
33. Smith JA, Ingram DJE (1962) Proc Phys Soc 80:139
34. Gordon DA, Marzke RF, Glaunsinger WS (1977) J Phys (Paris), Colloq 38:87
35. Sako SJ (1999) Phys Soc Jpn 59:1366
36. Dupree R, Forwood CT, Smith MJA (1967) Phys Stat Sol 24:525
37. Edmonds RN, Harrison MR, Edwards PP (1986) J Chem Soc Faraday Trans I 2515
38. Holland BW (1967) Conduction electron spin relaxation in small particles. In: Blinc R (ed) Magnetic resonance and relaxation: proceedings of the 14. Colloque Ampère, North-Holland, Amsterdam, pp 468–474
39. Honig A (1963) Paramagnetic relaxation in small particles. In: Low W (ed) Paramagnetic resonance: proceedings of the first international conference, Academic, New York, London, pp 439–442
40. Kawabata AJ (1970) Phys Soc Jpn 29:902
41. Kubo RJ (1962) Phys Soc Jpn 17:975
42. Marzke RF (1979) Catal Rev Sci Eng 19:43
43. Bandow S, Kimura K (1990) Sol State Commun 73:167
44. Lim HS, Ong CK (1992) Surf Sci 269/270:1109
45. Tosatti E, Ercolessi F (1991) Mod Phys Lett B 5:413
46. Urban J (1998) Cryst Res Technol 33:1009
47. Cleveland CL, Landman U (1991) J Chem Phys 94:11
48. Doye JPK, Calvo F (2001) Phys Rev Lett 86:3570
49. Gillet M (1977) Surf Sci 67:139
50. Ino S (1966) J Phys Soc Jpn 21:246
51. Sattler K (2002) The energy gap of clusters, nanoparticles, and quantum dots. In: Nalwa HS (ed) Handbook of thin film materials, vol 5. Academic, New York, pp 61–97
52. Lau JT, Achleitner A, Wurth W (2000) Chem Phys Lett 317:269
53. Palacios FJ, Iniguez MP, Lopez MJ, Alonso JA (1999) Phys Rev B 60:2908
54. Makov G, Nitzan A (1991) J Chem Phys 95:9024
55. Kappes MM, Schär M, Radi P, Schumacher E (1986) J Chem Phys 84:1863
56. Lang ND, Williams AR (1975) Phys Rev Lett 34:531
57. Wanner M, Kaim W, Lorenzen V, Preetz W (1999) Z Naturforsch 54b:1103
58. Lorenzen V, Preetz W, Baumann F, Kaim W (1998) Inorg Chem 37:4011
59. Binder H, Kellner R, Vaas K, Hein M, Baumann F, Wanner M, Winter R, Kaim W, Hönle W, Grin Y, Wedig U, Schultheiss M, Kremer RK, von Schnering HG, Groeger O, Engelhardt G (1999) Z Anorg Allg Chem 625:1059
60. Wanner M (2001) Ph.D. thesis, Universität Stuttgart
61. Sone J (1977) J Phys Soc Jpn 42:1457
62. Ashcroft NW, Mermin ND (1976) Solid State Physics. Saunders, New York, p 38
63. Beuneu F, Monod P (1978) Phys Rev B 18:2422